Hyperbiofilm Formation by *Bordetella pertussis* Strains Correlates with Enhanced Virulence Traits

Natalia Cattelan[1], Jamie Jennings-Gee[2], Purnima Dubey[3,4], Osvaldo M. Yantorno[1*] and Rajendar Deora[2,4*#]

[1]Centro de Investigación y Desarrollo en Fermentaciones Industriales (CINDEFI, CONICET-CCT-La Plata), Facultad de Ciencias Exactas, Universidad Nacional de La Plata, La Plata, Argentina.

[2]Department of Microbiology and Immunology, [3] Department of Pathology; Wake Forest School of Medicine, Winston-Salem, USA.

[4]The Department of Microbial Infection and Immunity; the Ohio State University Wexner Medical Center, Columbus, OH, USA

[*]Address correspondence to:
#Rajendar Deora, Ph.D.; Associate Professor: Rajendar.deora@osumc.edu
Osvaldo Yantorno, Ph.D: yantorno@quimica.unlp.edu.ar

[*]OMY and RD contributed equally to this work and have jointly supervised the work.

Running title: Hyperbiofilms and enhanced *Bordetella* pathogenesis

ABSTRACT

Pertussis or whooping cough caused by the obligate human pathogen *Bordetella pertussis* is undergoing a world-wide resurgence. Majority of studies with this pathogen are conducted with laboratory-adapted strains which may not be representative of the species as a whole. Biofilm formation by *B. pertussis* plays an important role in its pathogenesis. We conducted a side-by side comparison of the biofilm forming ability of the prototype laboratory strains with currently circulating isolates from two countries with different vaccination programs. Compared to the reference strain, all strains examined herein formed biofilms at higher levels. Biofilm structural analyses revealed country-specific differences with strains from USA forming more structured biofilms. Hyper bacterial aggregation and reciprocal expression of biofilm-promoting and inhibitory factors were observed in clinical isolates. An association of increased biofilm formation with augmented epithelial cell adhesion and higher levels of bacterial colonization in the mouse nose and trachea was detected. To our knowledge, this work links for the first time increased biofilm formation in bacteria with a colonization advantage in an animal model. We propose that the enhanced biofilm forming capacity of currently circulating strains contributes to their persistence, transmission and continued circulation.

INTRODUCTION

Bordetella pertussis is a human-restricted bacterial pathogen that causes whooping cough or pertussis. Pertussis has been re-emerging in industrialized countries and remains endemic in many parts of the world (1). Current pertussis vaccines while preventing the severe symptoms of the disease do not prevent colonization, transmission and circulation of the pathogen (2). Reasons suggested for the re-emergence of pertussis are: (i) heightened disease awareness; (ii) development of new clinical definitions; (iii) improved diagnostic ability; (iv) poor efficacy of the current commercial vaccines and (v) antigenic and genetic shifts in circulating strains (3).

Genetic changes in currently circulating strains of *B. pertussis* have been primarily observed in genes which encode vaccine antigens, such as pertussis toxin (PT), filamentous hemagglutinin (FHA), pertactin (PRN), and fimbriae (Fim2,3) (4-8). In addition, isolates deficient in the production of PRN, FHA and PT (9-11) and those showing increased production of PT have also been reported (12). These genetic and phenotypic alterations are hypothesized to confer an adaptive advantage to the circulating strains with respect to survival and transmission among vaccinated populations (12, 13). Based on these, it is proposed that the laboratory reference strains, after more than six decades of in-vitro passage, do not represent the circulating *B. pertussis* organisms (14). This accentuates the need for research on recently circulating strains not only with respect to uncovering genomic alterations but also on understanding phenotypic variations, an area that remains poorly studied.

Biofilms are sessile microbial communities which are enclosed in a self-produced or host-derived exopolymeric matrix (15). In some bacteria, biofilms promote environmental survival resulting in enhanced probability of host contact, while in others, biofilms are a critical

virulence determinant (16, 17). Many bacteria form biofilms during infection of non-mammalian and mammalian hosts and biofilms are in general less susceptible to anti-microbials and host immune components (18-20). Biofilms of *B. pertussis* have been observed on a variety of artificial surfaces and under static, shaking and fluid-flow conditions (21-25). Microscopically, *B. pertussis* biofilms are characterized by formation of spaced cell aggregates followed by the formation of three dimensional structures (pillars of bacteria separated by fluid channels or irregularly shaped microcolonies) encased in an opaque matrix composed of DNA and polysaccharide (23-27). In addition to laboratory settings, biofilms of *B. pertussis* have also been detected in the nose and trachea during experimental infections of mice (24, 25, 27). Correlation between biofilm forming ability of *B. pertussis* and pathogenesis is provided by the finding that mutants defective in biofilm formation on artificial surfaces fail to protect the bacterial cells from complement-mediated killing, attenuated for colonization of the mouse respiratory tract and are defective in biofilm formation on the respiratory tract (24, 27, 28). This has led to the hypothesis that biofilm formation in humans enables escape from immune defenses resulting in persistence, transmission and continued circulation of the bacteria (29). Support for this hypothesis is provided by microscopy of human tissue explants and respiratory tissues of patients which reveal biofilm-like structures similar to those formed on artificial surfaces and in mouse organs (30-32).

Very little is known about the mechanisms by which *B. pertussis* biofilm growth has adapted with respect to time, region and changing immunization regimens. While increased levels of biofilm formation by circulating strains from Argentina and Australia have been reported (33, 34), nothing is known about the biofilm forming ability of circulating isolates from the USA. It is also not known if there are differences in biofilm structure between strains from different countries. In this report, we performed a side-by side comparison of the biofilm forming

ability of currently circulating strains from the USA and Argentina with the objective of determining variations in biofilm forming capacity and structure. We have also examined the mechanistic bases for hyperbiofilm formation. Finally, we have investigated the relationship between enhanced biofilm formation and pathogenic phenotypes.

RESULTS

Recently circulating strains of *B. pertussis* from USA and Argentina form a thick bacterial ring at the air-liquid interface and display a hyperbiofilm phenotype

The biofilm forming ability of *B. pertussis* strains currently circulating in the USA is not known. During routine roller drum growth in glass tubes of one such strain (STO1-SEAT0004), we noticed a thick bacterial ring at the liquid–air interface. In comparison, the reference laboratory strains *B. pertussis* Tohama I and Bp536, a Tohama I derivative formed either a thinner ring or did not form a ring (Fig. 1A). We followed this observation with additional strains from the USA and Argentina and grew them side by side, for comparison purposes. The USA strains resulted in either compact rings at the air-liquid interface or diffused rings over the glass surface. For the strains that formed diffused rings (H973, S49560 and H897), very little bacterial growth was visible in the liquid phase (Fig. 1A). In comparison, all the Argentinean strains formed compact rings at the air-liquid interface.

We have previously reported a link between the formation of a ring at the air-liquid interface and biofilm formation in RB50, a *B. bronchiseptica* reference strain (35). Additionally, a cystic fibrosis isolate of *B. bronchiseptica* which formed a thicker ring than RB50, formed biofilms at higher levels (36). Thus, we hypothesized a hyperbiofilm phenotype for recent isolates of *B. pertussis*. To test this hypothesis, we quantified biofilms formed on polystyrene microtitre plates. After discarding bacteria from the planktonic phase and extensive washing, the attached biomass was quantified by staining adhered bacteria with crystal violet.

In comparison to Bp536 and BpTohama I, all recent isolates formed higher levels of biofilms on microtitre plates (Fig. 1C). The observed differences in biofilm levels cannot be

explained by enhanced growth, since none of the recent isolates displayed significantly higher growth in the planktonic phase of biofilm cultures compared to Bp536 (Fig. S1). In combination, these results suggest that recently circulating strains of *B. pertussis* form higher levels of biofilms than the model laboratory-adapted strains.

Hyperbiofilm forming strains display hyper aggregative properties

Very little is known about the mechanisms that contribute to hyperbiofilm formation in *B. pertussis*. A positive correlation between autoaggregation and biofilm formation has been reported in bacteria (36, 37). We compared the autoaggregation index (AI) of three randomly chosen recently circulating strains from Argentina (Bp462, Bp892 and Bp2751) and USA (H921, H973 and STO1-SEAT0004) with Bp536 (Fig. 2). AI represents the fraction of the aggregated bacterial cells. After two hours of static incubation, the AI of these six strains was 8 to 16-fold higher than that of Bp536. To determine the kinetics of cellular aggregation, the culture tubes were additionally incubated statically for 5 and 24h. While at 5 and 24h of incubation, the AI of Bp536was higher than that at 2h, it never reached the values observed for the clinical strains. For the clinical strains, there was not a significant increase in AI at 5 and 24h compared to that at 2h. We conclude that the clinical strains form cellular aggregates faster and at higher levels than the reference strain. These results suggest that the clinical strains utilize hyperaggregation as a means to enhance their biofilm forming capacity.

Recently isolated strains of *B. pertussis* display increased aggregation during initial surface attachment and form biofilms with enhanced structural complexity

The approaches used above do not provide detailed information on either the qualitative or quantitative strain-specific differences in biofilm structure. The objective of the next experiment was to conduct in situ visualization and analyses of differences in the biofilm 3D architecture of these strains. For this purpose, each of the six recently circulating strains and Bp536 was transformed with a GFP coding plasmid followed by culture on glass cover slips under agitating conditions and initial attachment and the biofilms formed were compared.

We first examined differences in initial attachment by incubating the strains on the substrate for 1h followed by microscopic observation. As shown in Fig. 3A, all six recently isolated strains adhered to the surface by forming aggregates, which were largely absent from Bp536. The formation of small clusters by these strains is consistent with their higher AI values. Quantification of bacteria attached to the glass cover slips revealed similar numbers of cells for all the strains including Bp536 (Fig. 3B). This suggests that the manner in which recently isolated strains attach to the surface is different than that of Bp536.

To observe and quantify the 3D structure of biofilms, the growth of biofilms was examined by Confocal Laser Scanning Microscopy (CLSM) at 24h intervals over a time period of 96h (Fig. 4). After 24h of growth, for Bp536, almost the entire surface area was completely covered with green cells which appeared to exist as a uniform monolayer. In contrast, all six recently isolated strains were present on the coverglass surface in the form of clustered cells and many areas of the coverglass were observed to be unoccupied. For theses strains, small pillars of cells, a characteristic architectural feature of *Bordetella* biofilms were also found (23, 27). At

48h of growth, while minute cell-clusters and thin pillars were observed for Bp536, the recently isolated strains continued to increase in thickness and cell density resulting in the visualization of thicker and more structured biofilms. After 72 and 96h of culture, while Bp536 achieved a more complex biofilm structure involving the formation of some water channels, the recently isolated strains continued to form complex biofilm structures with large and irregularly shaped clusters and longer cell pillars.

Interestingly, in addition to structural differences, region-specific variations in the biofilm features were also observed among the recently isolated strains. At time-points later than 24h, for the strains isolated in the USA (H921, H973 and STO1-SEAT0004), large and irregularly shaped cell aggregates continued to be observed during the entire time course of biofilm formation whereas for the Argentinean strains (Bp462, Bp892 and Bp2751) almost the entire surface area was green revealing a thick uniform layer of cells.

Quantitative analysis of biofilm architecture

In order to achieve a quantitative assessment of the observed microscopic differences in biofilm structure, CLSM-generated images were analyzed for four variables of biofilm architecture, biomass, maximum thickness, average thickness and roughness coefficient by the COMSTAT2 image analysis program (Fig. 5) (38). Overall, compared to Bp536 and at all time-points of biofilm formation, maximum thickness and average thickness were significantly higher for the recently isolated strains. The only exception was Bp892 for which, the maximum biofilm thickness was not significantly different from that of Bp536 at 24h. Biomass was significantly higher for all clinical isolates at 96h. The roughness coefficient, a measure of how much the biofilm thickness varies and thus a measure of biofilm heterogeneity varied the greatest between

Bp536 and the clinical strains. In general, for the Argentinean strains, the roughness coefficient was lower than Bp536 whereas for the USA strains it was higher at many of the time points. The differences in roughness coefficient between the Argentinean and USA strains correlated with microcolonies separated by empty spaces as observed by CSLM. Overall, these results suggest that the *B. pertussis* clinical strains form biofilms differently than the reference strain and differences in biofilm structure are observed between strains isolated from USA and Argentina.

Dispersal of biofilms by pronase E, DNase I and sodium metaperiodate.

Previously, we have shown that proteins, DNA and polysaccharides are components of the *B. pertussis* biofilm matrix and promote the stability of biofilms formed by Bp536 (21, 23-25). To address the functional roles of these components in stabilizing the biofilms of the recently isolated strains, we studied the effect of pronase E, DNase I and sodium metaperiodate ($NaIO_4$) on dispersal of pre-formed mature biofilms. Ninety-six hour old biofilms were incubated either with these reagents or with the respective buffer solutions for 2h at 37°C followed by CV staining to quantitate the stained biomass. Compared to Bp536, for five of the six recently isolated strains, pronase E treatment led to lower levels of biofilm dispersal (50.3% for Bp536 and varying between 25.3-32.3% for Bp462, Bp2751, H921, H973, STO1-SEAT0004, respectively). For the strain Bp892 however, pronase E treatment was sufficient to disperse the biofilms to similar levels as observed for Bp536 (Fig. 6A).

Sodium metaperiodate treatment resulted in two different levels of biofilm dispersal. For three of the recently isolated strains (Bp462, Bp2751 and H921), dispersion of biofilms was similar to that observed for Bp536 (varying between 31.7-37.6%). For the other three strains

(Bp892, H973 and STO1-SEAT0004) however, $NaIO_4$ treatment resulted in significantly higher levels (varying between 60.4-66.9%) of biofilm dispersal (Fig. 6B).

Similar to Bp536, for four of the recently isolated strains (Bp892, Bp2751, H973 and STO1-SEAT0004), greater than 50% of biofilms were dispersed by treatment with DNase I. For Bp892, incubation with DNase I led to greater than 85% dispersal. For two of the isolates (Bp2751 and Bp462), DNase I had somewhat of a moderate effect (35.4 and 40%, respectively) on biofilm dispersal (Fig. 6C). The varying levels of biofilm dispersal as a result of incubation with the above chemicals are probably because of the differences in biofilm formation between various strains. Taken together, these results suggest that similar to Bp536, recently isolated strains have protein, DNA and carbohydrate content in their biofilm matrix.

Recently isolated strains exhibit differential expression of *Bordetella* factors involved in biofilm formation and pathogenesis

Critical among factors that contribute to robust biofilm formation in *B. pertussis* are FHA, adenylate cyclase (AC) toxin and Bps polysaccharide (24, 27, 39). FHA and AC toxin promote and inhibit *B. pertussis* biofilm formation, respectively (24, 39). Bps is critical for the stability and maintenance of the three-dimensional structure of *B. pertussis* biofilms (27). In addition to their roles in biofilm formation, FHA, AC toxin and Bps also function as critical virulence factors for *B. pertussis* (27, 28, 40-42). Thus, we quantitated the expression levels of these factors in the clinical strains. As a negative control, the Bvg^- phase locked and the Δ*bps* strain were used. These strains do not express FHA and AC toxin and Bps, respectively.

We performed a whole-cell ELISA, to determine the levels of cell-surface associated FHA. As shown in Fig. 7A, compared to Bp536, all the recently isolated strains produced significantly

higher amounts (between 2.6 and 3.3-fold) of FHA. The expression of FHA was at background levels in this strain. As shown in Fig. 7B, compared to Bp536, all recent isolates displayed lower AC toxin activity.

Changes in the expression of the *bps* locus were determined by qRT-PCR by comparing levels of the *bpsA* transcript in Bp536 and the recently circulating strains. In two of the six recently isolates, expression of *bpsA* was significantly higher (5.4 and 1.6-fold higher in H921 and H973, respectively) (Fig. 7C). In four other strains, there were no significant differences in the expression levels of *bpsA* transcript. Bps production was detected by immunoblot in all of the recently isolated strains (Fig. 7D). Using ELISA, we failed to precisely and reproducibly quantitate Bps levels in the recently circulating isolates. Taken together, these results suggest that hyperbiofilm formation in recently isolated strains is associated with increased expression of genes/proteins that promote biofilm formation and decreased activity of the protein that inhibits biofilm formation.

Recently isolated strains exhibit hyper adhesion to respiratory epithelial cells of human origin

The recently isolated strains attached and formed higher levels of biofilms on artificial surfaces. Additionally, FHA was produced at higher levels in the clinical strains. FHA promotes the adherence of *B. pertussis* to epithelial cells (43). We hypothesized that compared to Bp536, the recently circulating strains will exhibit increased cellular adherence to epithelial cells. To test this hypothesis, we compared attachment of these strains to human alveolar epithelial cells (A549). As shown in Fig. 8, all the recently isolated strains adhered to A549 cells to a greater

extent than did Bp536. However, these differences in cellular attachment were statistically significant only for the strains Bp462, H973 and STO1-SEAT0004. As expected, the Bvg$^-$ phase locked strain which does not express FHA and other *Bordetella* adhesins exhibited very low levels of attachment to the epithelial cells.

Enhanced colonization of the mouse respiratory tract by recently isolated strains

To determine the role of hyperbiofilm phenotype in affecting the outcome of infection, we compared the colonization of Bp536 to the mouse respiratory tract to Bp462 and STO1-SEAT0004. Groups of eight to ten week old male and female mice were intranasally inoculated separately with the strains, and the bacterial loads of the nose, trachea and lungs were determined at 4 and 7 days post-inoculation (dpi) (Fig. 9). Consistent with previously published results, high bacterial loads of Bp536 were recovered from all three organs at 4 dpi (Fig. 9A). When compared to Bp536, while the two clinical strains colonized the nose and trachea at higher numbers at 4 dpi, no significant differences were found in bacterial numbers harvested from the lungs between any of the strains at this time point. At 7 dpi, all the three strains continued to colonize the respiratory organs at high numbers and the two recent isolates colonized the nose at higher numbers than Bp536 (Fig. 9B). Previously we have shown the existence of biofilms of *B. pertussis* in the mouse nose and trachea (24, 25, 27) and found that mutants defective in biofilm formation invitro are defective in colonization of the respiratory tract (24, 27). Thus, we propose that the observed hyperbiofilm phenotype of recent isolates contributes to the enhanced respiratory tract colonization.

DISCUSSION

Majority of studies on the biology and pathogenesis of the obligate human pathogen *B. pertussis* have been conducted with the strain BpTohama I and its derivatives. This strain originally isolated in Japan in the 1950s is a major source of pertussis vaccines. It has been suggested that it does not represent *B. pertussis* species (14). Although considerable effort is currently being dedicated towards genome sequencing and categorization of genomic differences between circulating clinical strains and domesticated laboratory strains, very little is known regarding their physiological and pathogenic differences. Biofilm formation is considered to be a survival strategy that allows enhanced respiratory tract colonization, persistence, transmission and circulation of *B. pertussis* in humans (24, 27-29). Characterization of the underlying molecular mechanisms, factors involved and the assessment of the relationship between biofilms and pathogenesis in currently circulating clinical isolates is important for the development of more effective vaccines and therapeutic alternatives to stem the resurgence of pertussis.

In this study, we utilized *B. pertussis* strains isolated during the period of 2001-2012 across two countries, Argentina and USA. While acellular vaccines are exclusively employed for immunization in the USA, whole-cell vaccines are used for the first five immunizations followed by the acellular vaccine as a booster for 11 year olds in Argentina. Despite having two different routine pertussis immunization programs, both these countries have experienced a steady increase in pertussis cases over the last decade. Thus, simultaneous comparison of recently circulating strains from these two countries is likely to shed light not only on variations in microbial pathogenic mechanisms but also on how bacterial pathogens evolve to evade and escape from vaccine-induced immunity.

In comparison to the reference strains, all the strains irrespective of the region and the year of isolation were characterized by hyperbiofilm formation. We propose that hyperbiofilm formation is a highly conserved strategy employed by *B. pertussis* for surface adherence and that this phenotype is maintained independent of the types of vaccines used for immunization.

The mechanisms underlying increased biofilm formation and strain-dependent differences in biofilm structure of *B. pertussis* was unknown until now. In this report, a positive correlation was found between hyper bacterial aggregation and enhanced biofilm formation in six of the selected currently circulating strains suggesting that both these processes depend on the same physical adhesive forces and that these strains may contain similar extracellular matrix that leads to enhanced cell-cell interactions. Structural analyses of biofilms by CLSM revealed significant regional differences in the biofilm architecture. In general, the Argentinean strains formed more compact and regularly shaped biofilms, while the USA strains developed distinct microcolonies and more structured and heterogeneous biofilms. The development of complex biofilm architecture has been linked to enhanced anti-microbial properties (44, 45). It remains to be determined if the differences in biofilm architecture between strains from USA and Argentina are due to bacterial adaptation to dissimilar vaccination programs and if these result in differential resistance to components of host immunity.

FHA and AC toxin have been shown to positively and negatively control biofilm formation in *B. pertussis*, respectively (24, 39). By promoting cell-surface and inter-bacterial adhesion, FHA promotes biofilm formation (24). AC toxin inhibits *B. pertussis* biofilm formation by directly interacting with FHA (39). We found an inverse correlation between FHA production and AC toxin activity in recently isolated clinical strains which were characterized by the production of higher levels of FHA and lower AC toxin activity. The observed differences in

FHA levels and AC toxin activity could also explain the hyperaggregating property of the clinical strains. FHA is responsible for autoaggregation in *B. pertussis* (46) and autoaggregation in *B. pertussis* is inhibited by addition of ACT (39). We propose that by inversely controlling the production of a biofilm inhibitory and promoting factor, the clinical strains are able to display higher levels of autoaggregation and biofilm formation. A similar link between production of FHA and AC toxin and hyperbiofilm formation was recently reported by us in a cystic fibrosis isolate of *B. bronchiseptica* which was characterized by higher expression of the *fhaB* and the absence of the *cyaA* gene from the genome (36). To our knowledge, this report is the first to document the lower AC toxin activity in recently circulating strains of *B. pertussis*. It will be highly informative to determine if this property is conserved in a larger number of strains and in strains isolated from other countries. The observed differences in the levels of FHA and AC toxin activity raise an interesting question regarding the mechanism by which the regulation of these two genes is maintained in the clinical strains.

The *Bordetella bpsABCD* locus required for the synthesis of the Bps polysaccharide is critical for the stability and maintenance of the complex architecture of biofilms (23, 47, 48). Compared to Bp536, two of the hyperbiofilm formers had higher levels of *bpsA* expression whereas in other four the expression of this gene was similar. All the strains produced Bps. Targeted mutagenesis will offer detailed insights on the relative contribution of individual genes in hyperbiofilm formation of these strains.

A striking result from the present study is the discovery of a link between hyperbiofilm forming ability of bacteria and enhanced pathogenic phenotypes. First, many of the hyperbiofilm forming strains from both Argentina and USA exhibited increased adherence to human epithelial cells. The increased cellular adherence of the recently isolated strains is most likely a direct

result of enhanced production of FHA. FHA facilitates attachment of *B. pertussis* to a variety of multiple cell types and extracellular structures in the respiratory epithelium (43, 49, 50).

Given the central role that biofilms play in promoting enhanced resistance to chemicals, antimicrobial compounds and components of host immunity, it is reasonable to hypothesize that a hyperbiofilm phenotype will result in better survival in host tissues and organs. A few studies have directly tested this hypothesis and the results obtained were generally not supportive. Bacterial mutants that display increased biofilm formation are either equally or significantly less virulent than wild type strains (51-57). Similarly, while the increased in vitro cellular adherence of the hyperbiofilm forming clinical strains should in theory lead to enhanced colonization in an animal model, previously we did not find this to be the case. A clinical strain of *B. bronchiseptica* despite exhibiting higher levels of biofilms and epithelial cell adherence than the laboratory strain was deficient in early colonization of the mouse respiratory tract (36). In this study, two of the recently isolated strains that displayed hyperbiofilm and hyper adherence phenotypes colonized the mouse nose and trachea at higher numbers. Whether the hyperbiofilm forming ability observed on artificial surfaces and higher bacterial numbers of the clinical strains in mouse nose and trachea correlate with quantitative and qualitative differences in nasal and tracheal biofilms needs to be determined.

In conclusion, we have for the first time demonstrated an association between higher levels of biofilm formation in bacteria with enhanced colonization in an animal model of infection. Based on the data obtained, we propose some mechanistic explanations for the continued circulation of *B. pertussis* and the resurgence of pertussis. Hyperaggregative, hyperbiofilm and hyper epithelial cell adhesive properties of the clinical strains most likely results in the formation of robust organ-adherent biofilm communities in the nose and trachea.

These biofilm-borne bacteria would survive better in the respiratory tract because of evasion of and escape from immune defenses leading to nasopharyngeal carriage. Droplet or airborne routes are principal ways of *B. pertussis* transmission. Efficient generation of and optimal particle size are critical determinates for successful host-host transmission. Droplets are generally defined as being ≥ 5 μm size and droplet sizes of diameters 30 μm of greater can remain suspended in the air. *B. pertussis* is a relatively small bacterium (0.4-0.8 μm) (58). We speculate that increased aggregation of the clinical strains in the respiratory tract could generate optimally-sized particles which will resist desiccation during transmission of infectious particles. Thus, a combination of enhanced respiratory tract survival followed by enhanced transmission has led to the resurgence of pertussis. Finally, the conservation of hyperbiofilm phenotype in *B. pertussis* strains in multiple continents with different vaccine and immunization schedules highlights the urgent need for continued research and development of alternative therapeutics and vaccines targeted towards the biofilm lifestyle.

MATERIALS AND METHODS

Ethics Statement

Housing, husbandry and experiments with animals were carried out in accordance with the guidelines approved by the Institutional Animal Care and Use Committee of Wake Forest School of medicine. Bacterial strains were collected by regional Microbiology Laboratories in Argentina and at Wake Forest School of Medicine as part of the patients' usual care, without any additional testing for the present investigation. De-identified organisms were provided to the investigators and the information received by the investigators was not individually identifiable. The research does not meet the federal definition of research involving human subject research as outlined in the federal regulations 45 CFR 46.

Strains and growth conditions

Strains used in this work are listed in Table 1. S49560 and M3984 were isolated in 2005 at WFSM from a 38 day old female baby (with coughing spells, apnea events and cyanosis) and a 7 week old female baby (with cough and respiratory distress), respectively. Argentinean strains were isolated at La Plata Children's Hospital (Hospital Interzonal de Agudos Especializado en Pediatría "Sor María Ludovica") and the patient ages varied between 6 and 16 weeks old. *B. pertussis* strains were maintained on Bordet-Gengou agar (BGA) supplemented with 10% v/v of defibrinated sheep blood. For liquid cultures, strains were grown in Stainer-Scholte (SS) broth (35, 59). *E. coli* strains were grown in Luria–Bertani medium. When appropriate, antibiotics

were added to maintain plasmids and for strain selection on agar plates, streptomycin, 50 μg mL^{-1}; kanamycin, 25 μg mL^{-1}; cephalexin, 40 μg mL^{-1}.

Biofilm formation assays

For microtitre dish assay of biofilm formation, 100 μL of bacterial suspension prepared at an OD_{650} of 1.0 were incubated statically for 4h at 37ºC. After this initial attachment step, medium was carefully removed, fresh SS medium was added and plates were incubated at 37ºC with shaking at 90 rpm. After every 24h of growth, medium was replaced with fresh SS medium. After indicated period of incubation, planktonic bacteria were removed and OD_{650} was measured. Adhered biomass was quantified by CV staining as previously described (60). Three independent experiments with quadruplicates for each strain were performed.

Autoaggregation assay

Bacteria were cultured in SS medium with heptakis (2,6-di-*O*-methyl-β-cyclodextrin) and supplement for 24h (61). Cells were harvested by centrifugation, washed and resuspended in only SS medium at an OD_{650} of 1.0 followed by static incubation at room temperature. At 2, 5 and 24h of incubation, 100μL of the medium was taken out from the top layer of the suspension and OD_{650} was measured. Autoaggregation index (AI) was calculated by $(OD_{t0}-OD_t)/OD_{t0}$, (where t0 is initial OD and t is OD measured at the designated time point). Three independent experiments were performed in duplicate for each sample. Statistical significance was evaluated by one-way ANOVA.

Transformation of *B. pertussis* strains with plasmidp GBSp1-GFP

B. pertussis strains were transformed by electroporation (62) of plasmid pGB5P1-GFP (63). Bacterial colonies were selected on BG agar containing kanamycin, and cultured in SS medium. GFP expression was confirmed by fluorescence microscopy.

Adhesion to abiotic surfaces

GFP-labeled strains were grown overnight in SS medium with kanamycin and used to prepare cell suspensions of OD_{650} of 0.2. Two mL of bacterial suspension was added to individual wells of 6 well cell culture plates containing coverglasses (22 x 22 mm) and after 1h of incubation at 37ºC, each well was washed twice with PBS. Coverglasses were mounted on glass slides with ProLong Gold antifade reagent (Invitrogen) and observed with a Nikon Eclipse microscope. Adhered cells were counted with ITCN plug-in (64), run by ImageJ (65). At least three independent experiments were performed by duplicate for each strain, where four random regions were chosen for bacterial counting.

Structural analysis of biofilms by CLSM

Biofilms were grown on 22 x 22 mm coverglasses in 6 well plates in SS medium supplemented with kanamycin. Each well was inoculated with a bacterial suspension at an OD_{650} of 1.0, followed by 4h of static incubation at 37°C, then the suspensions were removed and fresh medium was added. After every 24h of growth, the medium was replaced with fresh SS medium. Coverglasses were washed, mounted as described above, stored at 4°C for 24h and visualized with a Nikon Ti-Eclipse confocal microscope. Quantitative data corresponding to structural

features of the biofilms were acquired with COMSTAT2 (38). Each experiment was performed at least three times.

Enzymatic treatment of biofilms

Biofilms grown in microtitre plates for 96h were treated with DNase I (40 U) (25), pronase E (1 mg/mL) or sodium metaperiodate (40 mM, pH 5.0) for 2h at 37°C. Controls were treated with respective reaction buffers, 10 mM Tris-HCl pH 7.6, 2.5 mM $MgCl_2$, 0.5 mM $CaCl_2$ for DNase I; 10 mM Tris-HCl pH 7.5 for pronase E and with H_2O for sodium metaperiodate. After each enzymatic treatment, the remaining biofilm was quantified by staining with CV.

Enzyme-Linked Immunosorbent Assay (ELISA)

FHA production was determined by ELISA as previously described (66, 67). Briefly, 100 µL of heat-inactivated cells (OD_{650} of 0.05 for FHA) in PBS were added to strip plates (Corning EIA/RIA stripwell plate) and incubated overnight at 4ºC, washed with PBS buffer containing 0.05% Tween 20 (PBST) followed by blocking with 5% skim milk for 1h at 37ºC. A polyclonal serum raised in mouse (1:20,000 dilution) against purified FHA (Kaketsuken) was used as primary antibody. Antibody dilutions were prepared in 5% skim milk in PBST. As a control, non-immune serum was used. After 2h of incubation at 37ºC, plates were washed with PBST, the secondary antibody (HRP-conjugated goat anti-mouse IgG; 1:20,000 dilution) was added followed by incubation for 2h at room temperature. After washing with PBST, 100 µL of tetramethyl-benzidine (TMB, Sigma) was added to each well and incubated in dark for 20 min followed by addition of 1 MH_2SO_4 to stop the reaction. Absorbance was measured at 450 nm. For FHA protein quantification, a linear standard curve was prepared using different concentrations of purified FHA.

Quantitation of Adenylate cyclase enzymatic activity

B. pertussis clinical strains were grown to mid-log phase, until an OD_{650} of 0.7-0.8. AC activity was determined as previously reported (68).

RNA preparation, cDNA synthesis and qPCR

B. pertussis strains were grown under shaking conditions to an OD_{650} of 1.0, placed immediately on ice, centrifuged at 4°C and the bacterial pellets were lysed in RLT buffer (Qiagen). RNA was purified using the Qiagen RNeasy kit and treated with RQ1 DNase I (Promega) for 45 min at 37°C to obtain DNA-free RNA. cDNA was synthesized with random hexamers and SuperScriptIII reverse transcriptase (Invitrogen) as described earlier (69). Differential expression of genes between the strains Bp536, Bp462, Bp892, Bp2751, H921, H973 and STOI-SEAT0004 was analyzed by means of Pfaffl method (70), following real-time PCR quantification with SYBR Green. *rpoD* was used as a housekeeping gene for normalization. qPCR analysis was performed with three biological and two technical replicates. Primers used for qPCR are listed in Table 2.

Immunoblot analyses

Detection of Bps by Immunoblot was performed as previously described (23, 27). The membrane was probed with a 1:5,000 dilution of a goat antibody raised against *S. aureus* PNAG conjugated to diphtheria toxoid. The secondary antibody used was a horseradish peroxidase-conjugated mouse anti-goat immunoglobulin G (IgG) antibody (Pierce) diluted 1:20,000 and detected with the Amersham ECL (enhanced chemiluminescence) Western blotting system

476 **Bacterial adhesion to epithelial cells**

477 Human alveolar epithelial cells (A549) were cultured at 37°C under 5% CO_2 in Dulbecco's
478 modified Eagle's medium supplemented with 10% FBS and 4 mM of L-glutamine. A549 cells
479 were harvested at 90% confluency and approximately 2×10^5 cells were seeded in 24 well cell
480 culture plates followed by incubation overnight. 2×10^6 CFU of *B. pertussis* were added to the
481 wells, centrifuged at 900 rpm for 5 min to facilitate contact between bacteria and epithelial cells
482 followed by incubation at 37°C for 15 min to allow bacterial attachment to A549 cells. The
483 media was removed and the wells were washed four times with sterile PBS to remove any
484 nonattached bacteria. The eukaryotic cells were then lysed with 0.05% saponin and the mixture
485 was plated on BG-agar containing 10% blood and cephalexin for enumeration of attached
486 bacteria. Adhesion assays were performed by duplicate, three times.

487 **Animal experiments**

488 Housing, husbandry and experiments with animals were carried out in accordance with the
489 guidelines approved by the Institutional Animal Care and Use Committee of Wake Forest School
490 of medicine. Groups of (5-8) of 8-10 weeks old male and female C57BL/6 mice were used for all
491 the experiments. Mice were intranasally inoculated with 50 µl of a bacterial suspension with
492 approximately 5×10^5 CFU of the indicated *B. pertussis* strains. At 4 days post-infection, mice
493 were sacrificed followed by harvesting of nasal septum, trachea and three right lung lobes.
494 Tissues were homogenized in PBS containing 1% casein and plated on BG agar containing 10%
495 blood and streptomycin (for Bp536) or cephalexin (for clinical strains). After 3-5 days of growth
496 at 37°C colonies were enumerated. Statistical significance was determined by one-way ANOVA
497 and data were determined to be significant if $P< 0.05$.

ACKNOWLEDGEMENTS

We thank the Dr. Erik Hewlett and members of his laboratory for determining the levels of AC toxin and critical reading of the manuscript. Casandra Hoffman, Mary Gray and Erik Hewlett coordinated the samples, did the assays and reviewed the data, respectively. We are grateful to Dr. Gerry B. Pier for a gift of the PNAG-specific antibody. This project has been funded in part with Federal funds from the National Institute of Allergy and Infectious Diseases, National Institutes of Health, Department of Health and Human Services, under Contract No. HHSN272201200005C, R01AI125560 and 1R21AI123805-01; and funds from Agencia Nacional de Promoción Científica y Tecnológica (MINCYT, FONCYT, PICT 2012-2514) of Argentina. NC was supported by fellowships from CONICET and IUBMB (Wood-Whelan Research Fellowship)

FIGURE LEGENDS

FIG 1. Biofilm forming capacity of *B. pertussis* strains. (A) Formation of a bacterial ring at the air-liquid interface of glass culture tubes. (B) Microtitre assay of biofilm formation at 96h by *B. pertussis* strains. Each data point represents the average value of three independent experiments performed in quadruplicates; error bars indicate standard deviation. Significant differences were assessed by one-way ANOVA and Bonferroni posttest. Asterisks designate P values. **, <0.01 and ***, <0.001.

FIG 2. Quantification of autoaggregation of *B. pertussis* strains. Each bar represents the mean value of at least three independent experiments performed in duplicate. Error bars represent standard deviations. Statistical differences were assessed by one-way ANOVA and Bonferroni posttest. Asterisks designate P values. **, <0.01 and ***, <0.001.

FIG 3. Fluorescence microscopy and quantification of early bacterial attachment. (A) Attached GFP-labeled bacterial cells were observed by fluorescence microscopy. (B) Cells were counted by means of the ITCN plug-in, run by ImageJ. Data are average values of at least three independent experiments performed in duplicates. Four random regions were chosen for bacterial counting. Error bars indicate standard deviation.

FIG 4. CLSM micrographs of *B. pertussis* biofilms. GFP-labeled bacterial strains were grown on coverglasses in six well plates for the designated time points. Biofilms were visualized *in situ* by CLSM microscopy. CLSM image stacks were acquired at 0.9 µm z-intervals. Xy and xz representative focal planes are shown.

FIG 5. COMSTAT analyses of *B. pertussis* biofilms. CLSM image stacks were acquired at 0.9 µm z-intervals and analyzed by COMSTAT2. Average values of parameters from CLSM image

532 stacks derived from at least three independent experiments are shown with standard errors. P
533 values were determined using two-way ANOVA. (A) Average thickness and (B) Maximum
534 thickness; these values are calculated only on the biomass (without counting uncovered area).
535 (C) Biomass, this value represents the biomass volume divided by the area of the substratum. (D)
536 Roughness coefficient, this value represents the variability in the height of the biofilm.

537 **FIG 6.** Biofilm dispersal by matrix dissolving agents. Ninety six hour biofilms were treated with
538 pronase E in Tris buffer (A), 40 mM of sodium metaperiodate ($NaIO_4$) in H_2O (B) and DNase I
539 in reaction buffer (C) for 2 h at 37°C (black bars). Biofilms were treated with respective reaction
540 buffers as controls (white bars). Biofilm reduction is presented as percentage value of the
541 respective strain incubated with buffer only. Average values are shown from one representative
542 assay of three independent replicates, with their respective standard deviations. Significance was
543 assessed by two-way ANOVA, Asterisks designate *P* values. *, <0.05; **, <0.01 and ***,
544 <0.001.

545 **FIG 7.** Determination of the levels of biofilm associated factors/genes in *B. pertussis* strains. (A)
546 Cell-surface associated FHA determination by ELISA. Average values of three replicates are
547 presented with the respective standard deviation. (B) AC toxin activity quantification. AC toxin
548 levels were assessed by enzymatic activity (pmoles cAMP/10min/10µl/OD), as described earlier
549 (68). (C). *bpsA* expression and production. *bpsA* transcript levels were determined by qPCR and
550 Pfaffl method. Asterisks designate *P* values. *, <0.05; **, <0.01 and ***, <0.001. (D) Dot blot of
551 Bps. Production of Bps was detected as described previously (27).

552 **FIG 8.** Adherence of *B. pertussis* strains to epithelial cells. Adhesion assays were performed
553 with A549 epithelial cell lines. Each strain was incubated at a multiplicity of infection of 10.

554 Results are expressed as the proportion of adherent bacteria to the original inoculum. Each data
555 point is the average of three independent experiments performed in duplicate. Error bars indicate
556 the standard deviations. Statistical differences were assessed by one-way ANOVA ($p<0.0001$)
557 and the Student's t-Test with Bonferroni correction as post hoc. Asterisks designate *P* values. *,
558 <0.05, **, <0.01 and ***, <0.001.

559 **FIG 9.** Colonization of mouse respiratory tract by Bp536, Bp462 and STO1-SEAT0004. Groups
560 of C57BL/6 were intranasally inoculated with approximately 5×10^5 CFU in 50 µL of PBS. After
561 4 (A) and 7 days post-inoculation (B), animals were sacked and bacterial loads were determined
562 in nasal septum, trachea and lung. Horizontal bars represent the average value for each group.
563 Significance was analyzed by means of one-way ANOVA and Dunnett's posttest. Asterisks
564 designate P values. *, <0.05; **, <0.01 and ***, <0.001.

565

566

567 **TABLE 1**Strains used in this study.

Strains	Source	Year of isolation/reference
BpTohama I	Laboratory reference strain	1954
Bp536	Laboratory reference strain, Sm^r derivative of Tohama I	(71)
Bp369	(Bvg^-) derivative of Tohama III	(72)
Δ*fhaB*	Δ*fhaB* mutant	(73)
Δ*bps*	Δ*bps* mutant	(27)
Bp462	Argentina	2006
Bp479	Argentina	2007
Bp612	Argentina	2008
Bp892	Argentina	2007
Bp955	Argentina	2001
Bp1938	Argentina	2003
Bp2524	Argentina	2004
Bp2723	Argentina	2001
Bp2751	Argentina	2004
Bp2770	Argentina	2001
H918	USA	2012 (74)
H921	USA	2012 (74)
H973	USA	2012 (74)
H987	USA	2012 (74)
I002	USA	2012 (74)
STO1-CHOC0008	USA	2010 (74)
STO1-SEAT0004	USA	2011 (74)
M3984	USA	2005
S49560	USA	2005

568

569 **TABLE 2** Primer sequences

Primer	Sequence
rpoD-Fw	5´- ATGGGCATCCGCTTCACG
rpoD-Rv	5´- CTTCGTCCAACACCCAC
bpsA-Fw	5´- CGCTGCTGACCATGGATTT
bpsA-Rv	5´- CTGGTGTACAGCATGGTGTTGA

570

REFERENCES

1. Bart MJ, Harris SR, Advani A, Arakawa Y, Bottero D, Bouchez V, Cassiday PK, Chiang CS, Dalby T, Fry NK, Gaillard ME, van Gent M, Guiso N, Hallander HO, Harvill ET, He Q, van der Heide HG, Heuvelman K, Hozbor DF, Kamachi K, Karataev GI, Lan R, Lutynska A, Maharjan RP, Mertsola J, Miyamura T, Octavia S, Preston A, Quail MA, Sintchenko V, Stefanelli P, Tondella ML, Tsang RS, Xu Y, Yao SM, Zhang S, Parkhill J, Mooi FR. 2014. Global population structure and evolution of Bordetella pertussis and their relationship with vaccination. MBio 5:e01074.
2. Warfel JM, Zimmerman LI, Merkel TJ. 2014. Acellular pertussis vaccines protect against disease but fail to prevent infection and transmission in a nonhuman primate model. Proc Natl Acad Sci U S A 111:787-92.
3. Mooi FR, Van Der Maas NA, De Melker HE. 2014. Pertussis resurgence: waning immunity and pathogen adaptation - two sides of the same coin. Epidemiol Infect 142:685-94.
4. Packard ER, Parton R, Coote JG, Fry NK. 2004. Sequence variation and conservation in virulence-related genes of Bordetella pertussis isolates from the UK. J Med Microbiol 53:355-65.
5. van Amersfoorth SC, Schouls LM, van der Heide HG, Advani A, Hallander HO, Bondeson K, von Konig CH, Riffelmann M, Vahrenholz C, Guiso N, Caro V, Njamkepo E, He Q, Mertsola J, Mooi FR. 2005. Analysis of Bordetella pertussis populations in European countries with different vaccination policies. J Clin Microbiol 43:2837-43.
6. Kallonen T, Grondahl-Yli-Hannuksela K, Elomaa A, Lutynska A, Fry NK, Mertsola J, He Q. 2011. Differences in the genomic content of Bordetella pertussis isolates before and after introduction of pertussis vaccines in four European countries. Infect Genet Evol 11:2034-42.
7. Mooi FR, van Oirschot H, Heuvelman K, van der Heide HG, Gaastra W, Willems RJ. 1998. Polymorphism in the Bordetella pertussis virulence factors P.69/pertactin and pertussis toxin in The Netherlands: temporal trends and evidence for vaccine-driven evolution. Infect Immun 66:670-5.
8. van Loo IH, Heuvelman KJ, King AJ, Mooi FR. 2002. Multilocus sequence typing of Bordetella pertussis based on surface protein genes. J Clin Microbiol 40:1994-2001.
9. Pawloski LC, Queenan AM, Cassiday PK, Lynch AS, Harrison MJ, Shang W, Williams MM, Bowden KE, Burgos-Rivera B, Qin X, Messonnier N, Tondella ML. 2014. Prevalence and molecular characterization of pertactin-deficient Bordetella pertussis in the United States. Clin Vaccine Immunol 21:119-25.
10. Hegerle N, Paris AS, Brun D, Dore G, Njamkepo E, Guillot S, Guiso N. 2012. Evolution of French Bordetella pertussis and Bordetella parapertussis isolates: increase of Bordetellae not expressing pertactin. Clin Microbiol Infect 18:E340-6.
11. Williams MM, Sen K, Weigand MR, Skoff TH, Cunningham VA, Halse TA, Tondella ML. 2016. Bordetella pertussis Strain Lacking Pertactin and Pertussis Toxin. Emerg Infect Dis 22:319-22.
12. de Gouw D, Hermans PW, Bootsma HJ, Zomer A, Heuvelman K, Diavatopoulos DA, Mooi FR. 2014. Differentially expressed genes in Bordetella pertussis strains belonging to a lineage which recently spread globally. PLoS One 9:e84523.
13. Mooi FR, van Loo IH, van Gent M, He Q, Bart MJ, Heuvelman KJ, de Greeff SC, Diavatopoulos D, Teunis P, Nagelkerke N, Mertsola J. 2009. Bordetella pertussis strains with increased toxin production associated with pertussis resurgence. Emerg Infect Dis 15:1206-13.
14. Caro V, Bouchez V, Guiso N. 2008. Is the Sequenced Bordetella pertussis strain Tohama I representative of the species? J Clin Microbiol 46:2125-8.
15. Hall-Stoodley L, Costerton JW, Stoodley P. 2004. Bacterial biofilms: from the natural environment to infectious diseases. Nat Rev Microbiol 2:95-108.

16. Costerton JW, Cheng KJ, Geesey GG, Ladd TI, Nickel JC, Dasgupta M, Marrie TJ. 1987. Bacterial biofilms in nature and disease. Annu Rev Microbiol 41:435-64.
17. Parsek MR, Singh PK. 2003. Bacterial biofilms: an emerging link to disease pathogenesis. Annu Rev Microbiol 57:677-701.
18. Costerton JW, Stewart PS, Greenberg EP. 1999. Bacterial biofilms: a common cause of persistent infections. Science 284:1318-22.
19. Mah TF, O'Toole GA. 2001. Mechanisms of biofilm resistance to antimicrobial agents. Trends Microbiol 9:34-9.
20. Donlan RM, Costerton JW. 2002. Biofilms: survival mechanisms of clinically relevant microorganisms. Clin Microbiol Rev 15:167-93.
21. Bosch A, Serra D, Prieto C, Schmitt J, Naumann D, Yantorno O. 2006. Characterization of Bordetella pertussis growing as biofilm by chemical analysis and FT-IR spectroscopy. Appl Microbiol Biotechnol 71:736-47.
22. Serra D, Bosch A, Russo DM, Rodriguez ME, Zorreguieta A, Schmitt J, Naumann D, Yantorno O. 2007. Continuous nondestructive monitoring of Bordetella pertussis biofilms by Fourier transform infrared spectroscopy and other corroborative techniques. Anal Bioanal Chem 387:1759-67.
23. Parise G, Mishra M, Itoh Y, Romeo T, Deora R. 2007. Role of a putative polysaccharide locus in Bordetella biofilm development. J Bacteriol 189:750-60.
24. Serra DO, Conover MS, Arnal L, Sloan GP, Rodriguez ME, Yantorno OM, Deora R. 2011. FHA-mediated cell-substrate and cell-cell adhesions are critical for Bordetella pertussis biofilm formation on abiotic surfaces and in the mouse nose and the trachea. PLoS One 6:e28811.
25. Conover MS, Mishra M, Deora R. 2011. Extracellular DNA is essential for maintaining Bordetella biofilm integrity on abiotic surfaces and in the upper respiratory tract of mice. PLoS One 6:e16861.
26. Serra DO, Lucking G, Weiland F, Schulz S, Gorg A, Yantorno OM, Ehling-Schulz M. 2008. Proteome approaches combined with Fourier transform infrared spectroscopy revealed a distinctive biofilm physiology in Bordetella pertussis. Proteomics 8:4995-5010.
27. Conover MS, Sloan GP, Love CF, Sukumar N, Deora R. 2010. The Bps polysaccharide of Bordetella pertussis promotes colonization and biofilm formation in the nose by functioning as an adhesin. Mol Microbiol 77:1439-55.
28. Ganguly T, Johnson JB, Kock ND, Parks GD, Deora R. 2014. The Bordetella pertussis Bps polysaccharide enhances lung colonization by conferring protection from complement-mediated killing. Cell Microbiol 16:1105-18.
29. Cattelan N, Dubey P, Arnal L, Yantorno OM, Deora R. 2016. Bordetella biofilms: a lifestyle leading to persistent infections. Pathog Dis 74.
30. Mallory FB, Hornor AA. 1912. Pertussis: The histological Lesion in the Respiratory Tract. J Med Res 27:115-124 3.
31. Paddock CD, Sanden GN, Cherry JD, Gal AA, Langston C, Tatti KM, Wu KH, Goldsmith CS, Greer PW, Montague JL, Eliason MT, Holman RC, Guarner J, Shieh WJ, Zaki SR. 2008. Pathology and pathogenesis of fatal Bordetella pertussis infection in infants. Clin Infect Dis 47:328-38.
32. Soane MC, Jackson A, Maskell D, Allen A, Keig P, Dewar A, Dougan G, Wilson R. 2000. Interaction of Bordetella pertussis with human respiratory mucosa in vitro. Respir Med 94:791-9.
33. Arnal L, Grunert T, Cattelan N, de Gouw D, Villalba MI, Serra DO, Mooi FR, Ehling-Schulz M, Yantorno OM. 2015. Bordetella pertussis Isolates from Argentinean Whooping Cough Patients Display Enhanced Biofilm Formation Capacity Compared to Tohama I Reference Strain. Front Microbiol 6:1352.

34. Dorji D, Graham RM, Richmond P, Keil A, Mukkur TK. 2016. Biofilm forming potential and antimicrobial susceptibility of newly emerged Western Australian Bordetella pertussis clinical isolates. Biofouling 32:1141-1152.
35. Mishra M, Parise G, Jackson KD, Wozniak DJ, Deora R. 2005. The BvgAS signal transduction system regulates biofilm development in Bordetella. J Bacteriol 187:1474-84.
36. Sukumar N, Nicholson TL, Conover MS, Ganguly T, Deora R. 2014. Comparative Analyses of a Cystic Fibrosis Isolate of Bordetella bronchiseptica Reveal Differences in Important Pathogenic Phenotypes. Infect Immun 82:1627-37.
37. Silva-Dias A, Miranda IM, Branco J, Monteiro-Soares M, Pina-Vaz C, Rodrigues AG. 2015. Adhesion, biofilm formation, cell surface hydrophobicity, and antifungal planktonic susceptibility: relationship among Candida spp. Front Microbiol 6:205.
38. Heydorn A, Nielsen AT, Hentzer M, Sternberg C, Givskov M, Ersboll BK, Molin S. 2000. Quantification of biofilm structures by the novel computer program COMSTAT. Microbiology 146 (Pt 10):2395-407.
39. Hoffman C, Eby J, Gray M, Heath Damron F, Melvin J, Cotter P, Hewlett E. 2017. Bordetella adenylate cyclase toxin interacts with filamentous haemagglutinin to inhibit biofilm formation in vitro. Mol Microbiol 103:214-228.
40. Scheller EV, Cotter PA. 2015. Bordetella filamentous hemagglutinin and fimbriae: critical adhesins with unrealized vaccine potential. Pathog Dis 73:ftv079.
41. Masin J, Osicka R, Bumba L, Sebo P. 2015. Bordetella adenylate cyclase toxin: a unique combination of a pore-forming moiety with a cell-invading adenylate cyclase enzyme. Pathog Dis 73:ftv075.
42. Villarino Romero R, Osicka R, Sebo P. 2014. Filamentous hemagglutinin of Bordetella pertussis: a key adhesin with immunomodulatory properties? Future Microbiol 9:1339-60.
43. van den Berg BM, Beekhuizen H, Willems RJ, Mooi FR, van Furth R. 1999. Role of Bordetella pertussis virulence factors in adherence to epithelial cell lines derived from the human respiratory tract. Infect Immun 67:1056-62.
44. Lewis K. 2005. Persister cells and the riddle of biofilm survival. Biochemistry (Mosc) 70:267-74.
45. Stewart PS, Franklin MJ. 2008. Physiological heterogeneity in biofilms. Nat Rev Microbiol 6:199-210.
46. Menozzi FD, Boucher PE, Riveau G, Gantiez C, Locht C. 1994. Surface-associated filamentous hemagglutinin induces autoagglutination of Bordetella pertussis. Infect Immun 62:4261-9.
47. Sloan GP, Love CF, Sukumar N, Mishra M, Deora R. 2007. The Bordetella Bps polysaccharide is critical for biofilm development in the mouse respiratory tract. J Bacteriol 189:8270-6.
48. Nicholson TL, Brockmeier SL, Sukumar N, Paharik AE, Lister JL, Horswill AR, Kehrli ME, Jr., Loving CL, Shore SM, Deora R. 2017. The Bordetella Bps Polysaccharide Is Required for Biofilm Formation and Enhances Survival in the Lower Respiratory Tract of Swine. Infect Immun 85.
49. Tuomanen E, Weiss A, Rich R, Zak F, Zak O. 1985. Filamentous hemagglutinin and pertussis toxin promote adherence of Bordetella pertussis to cilia. Dev Biol Stand 61:197-204.
50. Bassinet L, Gueirard P, Maitre B, Housset B, Gounon P, Guiso N. 2000. Role of adhesins and toxins in invasion of human tracheal epithelial cells by Bordetella pertussis. Infect Immun 68:1934-41.
51. Mulcahy H, Lewenza S. 2011. Magnesium limitation is an environmental trigger of the Pseudomonas aeruginosa biofilm lifestyle. PLoS One 6:e23307.
52. Lin J, Cheng J, Chen K, Guo C, Zhang W, Yang X, Ding W, Ma L, Wang Y, Shen X. 2015. The icmF3 locus is involved in multiple adaptation- and virulence-related characteristics in Pseudomonas aeruginosa PAO1. Front Cell Infect Microbiol 5:70.

53. Ha R, Frirdich E, Sychantha D, Biboy J, Taveirne ME, Johnson JG, DiRita VJ, Vollmer W, Clarke AJ, Gaynor EC. 2016. Accumulation of Peptidoglycan O-Acetylation Leads to Altered Cell Wall Biochemistry and Negatively Impacts Pathogenesis Factors of Campylobacter jejuni. J Biol Chem 291:22686-22702.
54. de Bentzmann S, Giraud C, Bernard CS, Calderon V, Ewald F, Plesiat P, Nguyen C, Grunwald D, Attree I, Jeannot K, Fauvarque MO, Bordi C. 2012. Unique biofilm signature, drug susceptibility and decreased virulence in Drosophila through the Pseudomonas aeruginosa two-component system PprAB. PLoS Pathog 8:e1003052.
55. Goodman AL, Kulasekara B, Rietsch A, Boyd D, Smith RS, Lory S. 2004. A signaling network reciprocally regulates genes associated with acute infection and chronic persistence in Pseudomonas aeruginosa. Dev Cell 7:745-54.
56. Yi X, Yamazaki A, Biddle E, Zeng Q, Yang CH. 2010. Genetic analysis of two phosphodiesterases reveals cyclic diguanylate regulation of virulence factors in Dickeya dadantii. Mol Microbiol 77:787-800.
57. Candon HL, Allan BJ, Fraley CD, Gaynor EC. 2007. Polyphosphate kinase 1 is a pathogenesis determinant in Campylobacter jejuni. J Bacteriol 189:8099-108.
58. Gralton J, Tovey E, McLaws ML, Rawlinson WD. 2011. The role of particle size in aerosolised pathogen transmission: a review. J Infect 62:1-13.
59. Sukumar N, Sloan GP, Conover MS, Love CF, Mattoo S, Kock ND, Deora R. 2010. Cross-species protection mediated by a Bordetella bronchiseptica strain lacking antigenic homologs present in acellular pertussis vaccines. Infect Immun 78:2008-16.
60. Merritt JH, Kadouri DE, O'Toole GA. 2005. Growing and analyzing static biofilms. Curr Protoc Microbiol Chapter 1:Unit 1B 1.
61. Stainer DW, Scholte MJ. 1970. A simple chemically defined medium for the production of phase I Bordetella pertussis. J Gen Microbiol 63:211-20.
62. Zealey GR, Yacoob RK. 2000. Electrotransformation of Bordetella, p 150-156. *In* Eynard N, Teissié J (ed), Electrotransformation of Bacteria doi:10.1007/978-3-662-04305-9_18. Springer Berlin Heidelberg, Berlin, Heidelberg.
63. Weingart CL, Broitman-Maduro G, Dean G, Newman S, Peppler M, Weiss AA. 1999. Fluorescent labels influence phagocytosis of Bordetella pertussis by human neutrophils. Infect Immun 67:4264-7.
64. Byun J, Verardo MR, Sumengen B, Lewis GP, Manjunath BS, Fisher SK. 2006. Automated tool for the detection of cell nuclei in digital microscopic images: application to retinal images. Mol Vis 12:949-60.
65. Schneider CA, Rasband WS, Eliceiri KW. 2012. NIH Image to ImageJ: 25 years of image analysis. Nat Methods 9:671-5.
66. Barkoff AM, Guiso N, Guillot S, Xing D, Markey K, Berbers G, Mertsola J, He Q. 2014. A rapid ELISA-based method for screening Bordetella pertussis strain production of antigens included in current acellular pertussis vaccines. J Immunol Methods 408:142-8.
67. Tsang RS, Sill ML, Advani A, Xing D, Newland P, Hallander H. 2005. Use of monoclonal antibodies to serotype Bordetella pertussis isolates: comparison of results obtained by indirect whole-cell enzyme-linked immunosorbent assay and bacterial microagglutination methods. J Clin Microbiol 43:2449-51.
68. Eby JC, Gray MC, Warfel JM, Paddock CD, Jones TF, Day SR, Bowden J, Poulter MD, Donato GM, Merkel TJ, Hewlett EL. 2013. Quantification of the adenylate cyclase toxin of Bordetella pertussis in vitro and during respiratory infection. Infect Immun 81:1390-8.

69. Conover MS, Redfern CJ, Ganguly T, Sukumar N, Sloan G, Mishra M, Deora R. 2012. BpsR modulates Bordetella biofilm formation by negatively regulating the expression of the Bps polysaccharide. J Bacteriol 194:233-42.
70. Pfaffl MW. 2001. A new mathematical model for relative quantification in real-time RT-PCR. Nucleic Acids Res 29:e45.
71. Stibitz S, Yang MS. 1991. Subcellular localization and immunological detection of proteins encoded by the vir locus of Bordetella pertussis. J Bacteriol 173:4288-96.
72. Weiss AA, Falkow S. 1984. Genetic analysis of phase change in Bordetella pertussis. Infect Immun 43:263-9.
73. Carbonetti NH, Artamonova GV, Andreasen C, Dudley E, Mays RM, Worthington ZE. 2004. Suppression of serum antibody responses by pertussis toxin after respiratory tract colonization by Bordetella pertussis and identification of an immunodominant lipoprotein. Infect Immun 72:3350-8.
74. Harvill ET, Goodfield LL, Ivanov Y, Meyer JA, Newth C, Cassiday P, Tondella ML, Liao P, Zimmerman J, Meert K, Wessel D, Berger J, Dean JM, Holubkov R, Burr J, Liu T, Brinkac L, Kim M, Losada L. 2013. Genome Sequences of 28 Bordetella pertussis U.S. Outbreak Strains Dating from 2010 to 2012. Genome Announc 1.

A

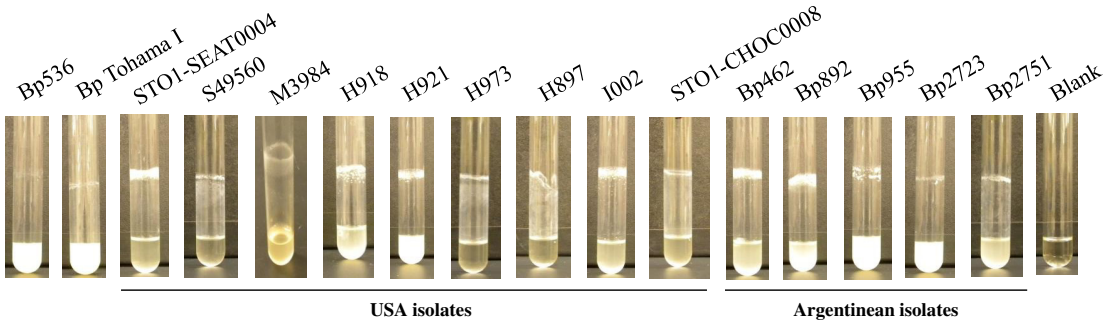

B

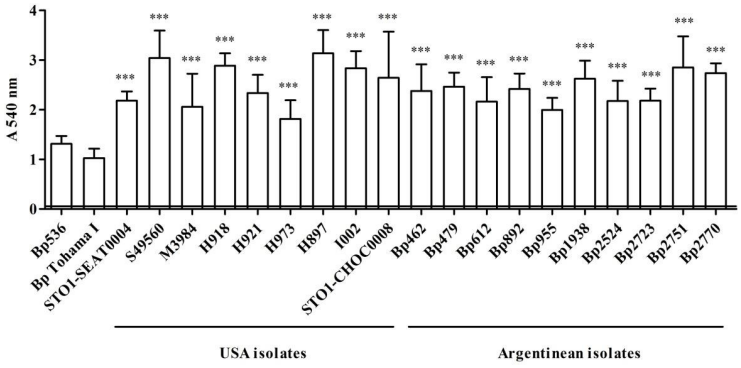

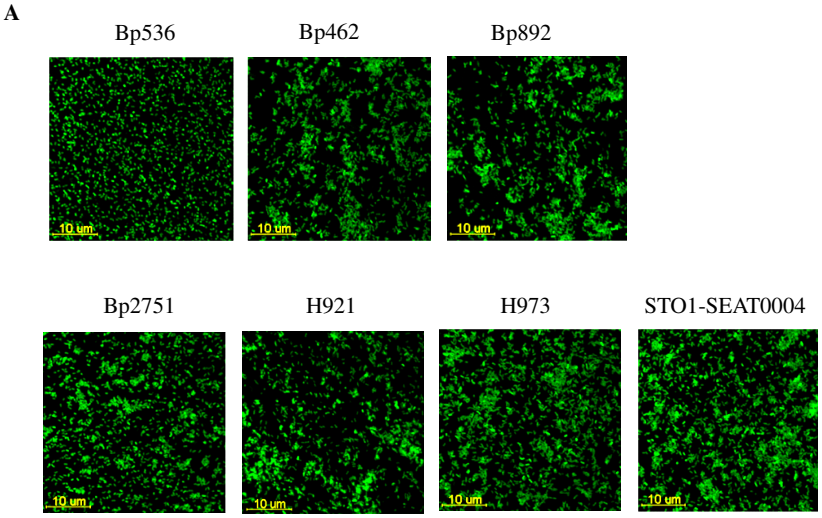

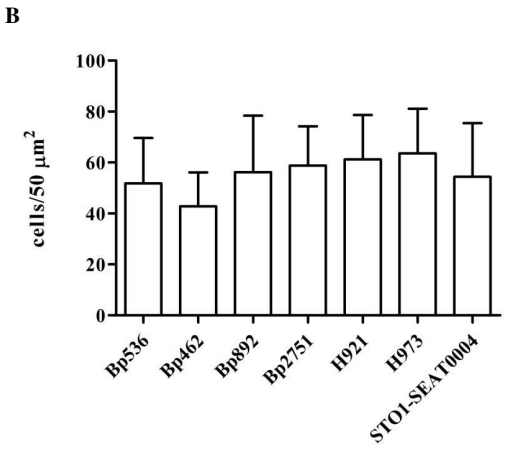

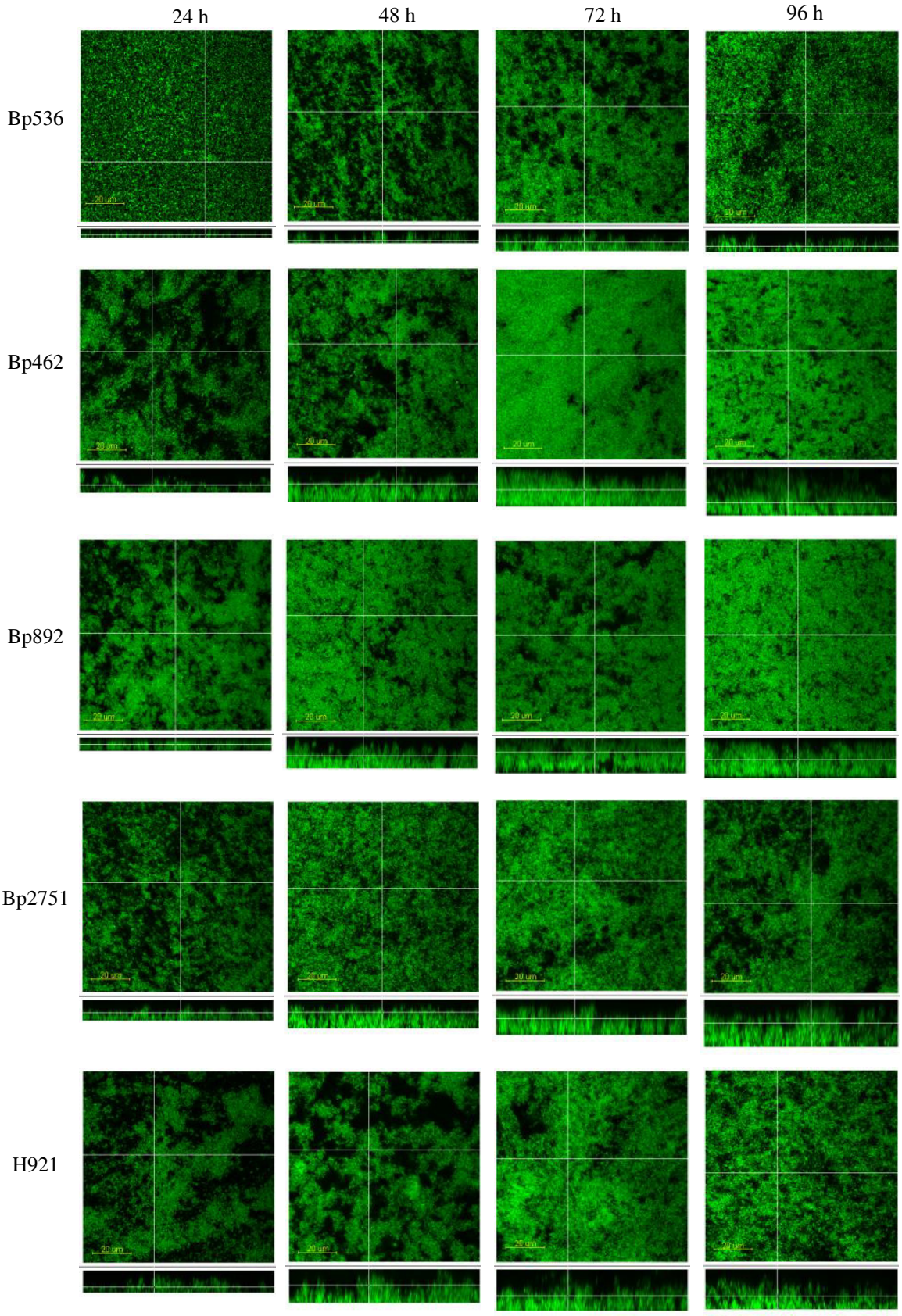

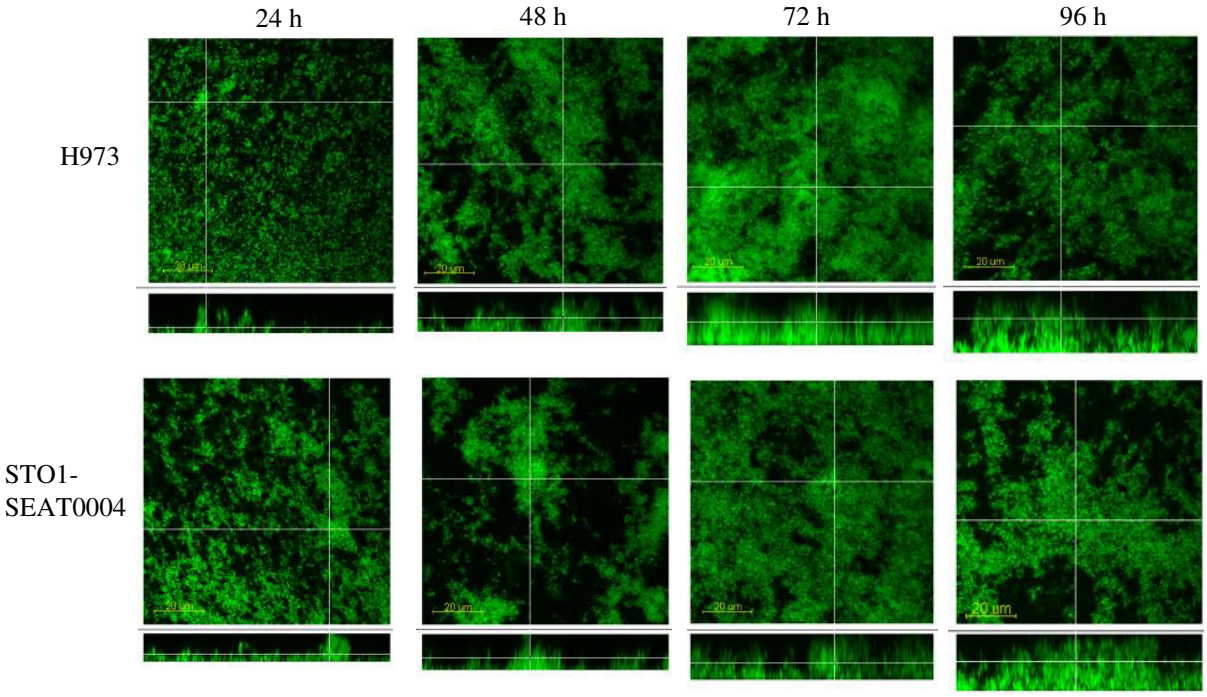

Infection and Immunity
IAI
Infection and Immunity